Molecular Pharmacology Fast Forward. Published on July 26, 2011 as DOI: 10.1124/mol.111.071381
This article has not been copyedited and formatted. The final version may differ from this version.
Molecular Pharmacology Fast Forward. Published on July 26, 2011 as doi: 10.1124/mol.111.071381

Aryl hydrocarbon receptor activation in hematopoietic stem/progenitor cells alters cell function and pathway-specific gene modulation reflecting changes in cellular trafficking and migration

Fanny L. Casado, Kameshwar P. Singh, Thomas A. Gasiewicz

Department of Environmental Medicine, University of Rochester Medical Center, Rochester, New York

Downloaded from molpharm.aspetjournals.org at ASPET Journals on April 17, 2024

Copyright 2011 by the American Society for Pharmacology and Experimental Therapeutics.

Molecular Pharmacology Fast Forward. Published on July 26, 2011 as DOI: 10.1124/mol.111.071381
This article has not been copyedited and formatted. The final version may differ from this version.

AhR activation alters migration of hematopoietic stem cells

Corresponding author: Thomas A. Gasiewicz, Ph.D.

Department of Environmental Medicine, University of Rochester, School of Medicine and Dentistry, Box-EHSC, 601 Elmwood Avenue, Rochester, NY 14642.

Phone: (585) 275-3265, Fax: (585) 256-2591.

Email: **Tom_Gasiewicz@urmc.rochester.edu**

Downloaded from molpharm.aspetjournals.org at ASPET Journals on April 17, 2024

Number of Text Pages: 36

Number of Tables: 2

Number of Figures: 5

Number of References: 38

Number of Words:

Abstract: 256

Introduction: 531

Discussion: 1,487

Non-standard abbreviations:

7-amino-actinomycin D, 7AAD;

Allophycocyanin, APC;

Aryl hydrocarbon Receptor, AhR;

Bone Marrow, BM;

Chemokine (C-X-C motif) Ligand 12, Cxcl12;

Competitive Repopulation Units, CRU;

Fluorescein, FITC;

Hematopoietic Stem Cells, HSCs;

Ingenuity Pathway Analysis, IPA;

Lineage depleted, Sca-1$^+$ and c-kit$^+$ cells, LSKs;

Multi-experiment Viewer, MeV;

Multi-potent progenitor, MPP;

Per-ARNT-Sim, PAS;

Phycoerythrin, PE;

Real-time Reverse Transcription Polymerase Chain Reaction, RT^2-PCR;

Signaling Lymphocyte Activation Molecules, SLAM;

Stem cell factor, Scf;

2,3,7,8-tetrachlorodibenzo-p-dioxin, TCDD;

University of Rochester Medical Center, URMC.

Molecular Pharmacology Fast Forward. Published on July 26, 2011 as DOI: 10.1124/mol.111.071381
This article has not been copyedited and formatted. The final version may differ from this version.

Abstract

The aryl hydrocarbon receptor (AhR) is a transcription factor belonging to the Per-ARNT-Sim family of proteins. These proteins sense molecules and stimuli from the cellular/tissue environment, and initiate signaling cascades to elicit appropriate cellular responses. Recent literature suggests an important function of AhR in hematopoietic stem cell (HSC) biology. However, the molecular mechanisms by which AhR signaling regulates HSC functions are unknown. In previous studies, we and others reported that treatment of mice with the AhR agonist 2,3,7,8-tetrachlorodibenzo-p-dioxin (TCDD) compromises the competitive reconstitution of bone marrow (BM) cells into irradiated host animals. Additional studies indicated a requirement for AhR in hematopoietic cells and not marrow microenvironment cells. In this study, we tested the hypothesis that TCDD-mediated phenotypic and functional changes of HSCs are a result of changes in gene expression that disrupt stem cell numbers and/or their migration. TCDD treatment to mice increased the numbers of phenotypically-defined HSCs in BM. These cells showed compromised migration to the BM *in vivo* and to the chemokine CXCL12 *in vitro*, as well as increased expression of the leukemia-associated receptors CD184(CXCR4) and CD44. Gene expression profiles at six and twelve h after exposure were consistent with the phenotypic and functional changes observed. The expression of *Scin, Nqo1, Flnb, Mmp8, Ilf9, and Slamf7* were consistently altered. TCDD also disrupted expression of other genes involved in hematological system development and function including *Fos, JunB, Egr1, Ptgs2*(*Cox2*) and *Cxcl2.* These data support a molecular mechanism for an AhR ligand to disrupt the homeostatic cell signaling of HSCs that may promote altered HSC function.

Downloaded from molpharm.aspetjournals.org at ASPET Journals on April 17, 2024

Molecular Pharmacology Fast Forward. Published on July 26, 2011 as DOI: 10.1124/mol.111.071381
This article has not been copyedited and formatted. The final version may differ from this version.

Introduction

The aryl hydrocarbon receptor (AhR) is a basic helix-loop-helix protein belonging to the Per-ARNT-Sim (PAS) superfamily of proteins. Physiologically, many of the PAS proteins sense molecules and stimuli from the cellular/tissue environment, and initiate signaling cascades to elicit appropriate cellular responses. Lipophilic compounds such as halogenated and polycyclic aromatic hydrocarbons, including the potent exogenous ligand 2,3,7,8-tetrachlorodibenzo-p-dioxin (TCDD) (Poland and Glover 1973), bind to the cytoplasmic AhR leading to a sequence of conformational changes that ultimately transform the AhR into its high-affinity DNA binding form in the nucleus to function as a transcription factor (Soshilov and Denison 2008) .

Epidemiological data has correlated accidental and occupational exposure to TCDD and related dioxins with increased risk for certain hematological diseases such as non-Hodgkin's lymphoma, chronic lymphocytic leukemia and multiple myeloma in humans (Frumkin, 2003). Also, there is much data indicating that persistent activation of AhR results in immuno-suppression in different animal models (Stevens, et al., 2009). AhR-dependent thymic atrophy, a hallmark of exposure to varying doses of TCDD, may be elicited by different mechanisms including (1) reduced seeding of the thymus by bone marrow (BM)-derived progenitors (Fine, et al., 1990), (2) reduced stromal-mediated proliferation of thymocytes (Kremer, et al., 1994; Frericks, et al., 2007), and (3) a skewing of the thymic output through direct effects on developing thymocytes (Laiosa, et al., 2010). Additionally, AhR activation leads to (1) alterations of B lineage cells during gestation with possible consequences on autoimmunity (Mustafa, et al., 2008), (2) decreased numbers of immature B cells (Murante and Gasiewicz, 2000), and (3) altered functional activity of early hematopoietic progenitors (Murante and Gasiewicz, 2000; Sakai, et al., 2003; Singh, et al., 2009). A single dose of TCDD that results in BM TCDD concentrations of < 1 nM (Fine, et al., 1990) increases the relative numbers of phenotypically-defined HSCs/progenitors (Staples, et al., 1998) starting 2 days post-treatment and lasting until

Downloaded from molpharm.aspetjournals.org at ASPET Journals on April 17, 2024

Molecular Pharmacology Fast Forward. Published on July 26, 2011 as DOI: 10.1124/mol.111.071381
This article has not been copyedited and formatted. The final version may differ from this version.

day 31 (Murante and Gasiewicz, 2000). Furthermore, TCDD-treated phenotypically-defined long-term HSCs were unable to sustain peripheral blood repopulation (Sakai, et al., 2003), and had compromised ability to competitively repopulate the BM of irradiated mice (Singh, et al., 2009). These effects were dependent on the presence of the AhR in hematopoietic cells, but not supporting stroma (Staples, et al. 1998; Sakai, et al. 2003). Together, these data support a hypothesis that primitive progenitors of hematopoiesis in the BM are targeted by AhR-ligands resulting in AhR-mediated phenotypic and functional changes. Given recent interest in the possible use of AhR ligands for the expansion of HSCs and their use in BM transplants (Boitano, et al., 2010), as well as treatment of autoimmune disease (Quintana, et al., 2010), it is critical to further define mechanisms related to effects on hematopoietic cell function and the signaling pathways that may mediate these alterations.

This work tests the hypothesis that TCDD- and AhR-mediated phenotypic and functional changes of murine HSCs are a consequence of disruption of stem cell numbers and/or their migration preceded by changes in gene expression. Understanding these changes in gene expression and their functional consequences in HSCs may provide a rationale to define a role of AhR in HSCs. Furthermore, this information may provide avenues to further explore the use of therapeutic AhR ligands.

Downloaded from molpharm.aspetjournals.org at ASPET Journals on April 17, 2024

Molecular Pharmacology Fast Forward. Published on July 26, 2011 as DOI: 10.1124/mol.111.071381
This article has not been copyedited and formatted. The final version may differ from this version.

Materials and Methods

Mice and Treatments

Five-week old C57BL/6J female mice were purchased from The Jackson Laboratories (Bar Harbor, ME) and housed in the facilities of the University of Rochester Medical Center (URMC) (Singh, et al., 2009) for at least a week before treatment. CD45.1$^+$ (B6.SJL-Ptprc<a>/BoAiTac) female mice used in repopulation experiments were purchased from Taconic Farms Inc (Germantown, NY).

TCDD was obtained from Cambridge Isotopes (Andover, MA) and 6 μg/mL aliquots were prepared as previously described (Laiosa, et al., 2010). Either 30 μg of TCDD in olive oil/kg body weight or olive oil alone in a volume of 0.1 mL/20 g body weight was given orally by gavage. Mice were euthanized after 7 days for functional and phenotypic experiments. This dose and time were chosen based on determined optimal effects of TCDD on HSCs (Singh, et al., 2009). To study gene expression, treated mice were euthanized 6 and 12 hours after treatment.

Cell Preparations

Bone marrow (BM) was harvested from femurs and tibias, red blood cells were lysed, and lineage positive leukocytes were depleted as previously described (Singh, et al., 2009). Only cell suspensions with viability > 95% as measured by exclusion of Trypan blue were used for further experimentation. All flow cytometric analyses and separations were performed on viable populations only, as measured by exclusion of the fluorescent dye 7-amino-actinomycin D (7AAD). Lineage depleted Sca-1$^+$ and c-kit$^+$ cells (LSKs) used in microarray experiments were obtained by laser-assisted sorting of lineage depleted cells stained with fluorochrome-conjugated antibodies against Sca-1$^+$ (D7, allophycocyanin (APC); ebioscience, San Diego, CA) and c-kit$^+$ (2B8, fluorescein (FITC); BD Pharmingen, Santa Clara, CA) using a FACSAria cell

Downloaded from molpharm.aspetjournals.org at ASPET Journals on April 17, 2024

Molecular Pharmacology Fast Forward. Published on July 26, 2011 as DOI: 10.1124/mol.111.071381
This article has not been copyedited and formatted. The final version may differ from this version.

sorter (BD Biosciences, San Jose, CA) and a gating scheme recently published (Singh, et al., 2010). To examine differentiation of LSK cells under conditions *in vitro*, LSK cells were obtained from mice treated with TCDD (30 μg/kg, 7d) or vehicle. Thirty thousand cells (10,000 cells/mL) were cultured per well in 12-well plates. Each well contained StemSpan Serum-Free Expansion Media (Stem Cell Technologies) supplemented with IL-6 (50 ng/mL) or IL-6 plus stem cell factor (Scf) (100 ng/mL). Cells were harvested after 7 d or 14d and phenotypic characterization was performed by flow cytometry.

Determination of Competitive Repopulation Units

The engraftment and proportion of Competitive Repopulation Units (CRU), per million of donor's BM cells injected into the irradiated recipients, were calculated for short-term and long-term reconstitutions (6 and 20 weeks post-transplantation, respectively). A limiting-dilution approach was used for quantification. BM cells were isolated from control or TCDD-treated mice. The donor's ($CD45.2^+$) cells were resuspended in 100 μL of PBS at three concentrations (0.1, 0.2, and 1 x 10^6) and mixed with 100 μL of PBS containing 2 x 10^5 competitive donor's ($CD45.1^+$) BM cells. Recipient ($CD45.1^+$) mice were irradiated with two doses of 5.5 Gy from a Cesium source. Mixtures of donor and competitive donor cells were injected intravenously in eight recipients. After 6 (short-term) or 20 (long-term) weeks post-transplantation, recipients were sacrificed and BM cells were isolated. BM cells were stained using commercially fluorochrome-conjugated antibodies against CD45.1 (A20, APC; BD Pharmingen) and CD45.2 (104, FITC; BD Pharmingen), and analyzed using a FACSCanto (BD Biosciences) flow cytometer. Engraftment of the progeny was evaluated based on the percentages of donor-derived $CD45.2^+$ BM cells. For the limiting-dilution analysis, the presence of more than 1% cells of donor origin ($Cd45.2^+$) was considered as positive engraftment. The proportions of HSCs per million BM cells were calculated assuming a single-hit Poisson statistics (Purton and Scadden, 2007) and using the L-Calc software (StemCell Technologies, Vancouver, Canada).

Downloaded from molpharm.aspetjournals.org at ASPET Journals on April 17, 2024

Molecular Pharmacology Fast Forward. Published on July 26, 2011 as DOI: 10.1124/mol.111.071381
This article has not been copyedited and formatted. The final version may differ from this version.

Migration of Hematopoietic Precursors

The *in vivo* migration of hematopoietic precursors was examined 24 hours after i.v. injection. Two hundred and fifty μL of sterile PBS containing 5 million TCDD- or vehicle-treated donor BM cells were injected in the tail vein of non-irradiated recipients. The number of BM cells used was optimized experimentally, and represents about 6.3% of the total number of BM cells in WT mice (i.e. recipients). The migration of phenotypically-defined HSCs/progenitors was calculated as the ratio of the numbers of $CD45.2^+$ LSK cells retrieved from transplanted recipients per the numbers of $CD45.2^+$ donor LSK cells injected.

The *in vitro* migration was studied utilizing a transwell assay. One hundred and fifty μL of the chemo-attractant murine chemokine (C-X-C motif) ligand 12 (CXCL12), also known as stromal-derived factor-1α (Miltenyi Biotech, Bergisch Gladbach, Germany) was added to each well of a V-bottom 96-well plate (BD, Franklin Lakes, NJ) at concentrations of 0, 50, 100 or 300 ng/mL. The HTS Transwell 96 Permeable support with a 5 μm polycarbonate membrane (Corning Life Sciences, Lowell, MA) was placed on top of the plate containing chemo-attractant. Five hundred thousand of lineage depleted (Lin^-) cells resuspended in 50 μL of PBS were placed on top of the permeable support and incubated at 37°C, for 3 hours at 5% CO_2. To determine migration, cells that were recovered from the bottom well were stained with 7AAD, and fluorochrome-conjugated antibodies against Sca-1 and c-kit.

Phenotyping of Cells

Flow cytometry was performed using a LSR-II flow cytometer (BD Biosciences) in the Flow Core Facility of the URMC, and was used to phenotypically define long-term and short-term HSCs (Kiel, et al., 2005) using fluorochrome-conjugated antibodies against CD48 (HM48-1, Phycoerythrin (PE)-Cy7, BD Pharmingen) and CD150 (9D1, APC; ebioscience). LSK cells (Sca-1 (E13-161.7, APC; BD Pharmingen) and ckit (2B8, PE-Cy5; BD Pharmingen)) were

Downloaded from molpharm.aspetjournals.org at ASPET Journals on April 17, 2024

Molecular Pharmacology Fast Forward. Published on July 26, 2011 as DOI: 10.1124/mol.111.071381
This article has not been copyedited and formatted. The final version may differ from this version.

phenotyped for the expression of markers involved in the interactions between HSCs and their microenvironment such as: the integrin dimer α4β1 (also, Very Late Antigen-4) composed of CD49d (also α4; R1-2, PE; BD Pharmingen) and CD29 (also β1; Ha2/5, FITC; BD Pharmingen), CD184 (2B11/CXCR4, APC; BD Pharmingen), CD44 (IM7, PE-Cy5; BD Pharmingen), and CD162 (also P-selectin glycoprotein ligand-1; 2PH1, PE, BD Pharmingen). Flow cytometric analysis was performed in viable cells excluding 7AAD. For apoptosis analysis, Lin- cells were incubated with fluorochrome-conjugated antibodies against ckit (2B8, APC) and Sca-1 (D7, V450). Cells were washed and resuspended in 1X Annexin V Binding Buffer (BD Pharmingen), and then incubated with 7AAD and Annexin V-PE according to manufacturer's recommendations. 7AAD and Annexin V double-negative cells were gated as viable cells, and 7AAD negative and Annexin V positive cells were gated as apoptotic cells. Unstained, single fluorochrome and all-fluorochromes-except-one were used to compensate the fluorescent signals. Data were calculated and plotted using FlowJo software (Tree Star Inc., Ashland, OR).

Microarray Experiments

Total RNA was isolated from sorted LSK cells pooled from 20 mice using RNeasy Mini/Micro Kit (Qiagen, Valencia, CA), DNAse treated, and quantified using the ND-1000 spectrophotometer (NanoDrop Technologies, Wilmington, DE). Microarray analyses were done according to standard operating procedures by the Functional Genomics Center at the URMC. RNA quality was confirmed by the presence of two peaks on a 2:1 ratio of intensity of 28S:18S rRNA using an Agilent 2100 Bioanalyzer (Agilent Technologies Inc., Santa Clara, CA). RNA (20 ng) was amplified using the NuGEN Ovation RNA Amplification System (San Carlos, CA) to yield single stranded cDNA, then hybridized with the GeneChip® Mouse Gene 1.0 ST Array (Affymetrix, Santa Clara, CA). Five microarrays from independent RNA preparations per treatment were used. The microarrays were processed as previously described (Henry, et al., 2010). The relative fold-changes of the signal intensity averages of TCDD with respect to control at the 6 h

Downloaded from molpharm.aspetjournals.org at ASPET Journals on April 17, 2024

Molecular Pharmacology Fast Forward. Published on July 26, 2011 as DOI: 10.1124/mol.111.071381
This article has not been copyedited and formatted. The final version may differ from this version.

and 12 h time-points were calculated for each of the 35,556 probes. Assuming a normal distribution of the data, the F-test was performed to evaluate variances between the treated and control group, and calculate the p-value obtained after performing the two-tailed Student's T-test using Microsoft Excel.

Gene-specific Primers and Real-time Reverse-transcription (RT^2-PCR)

Gene-specific primers and real-time reverse-transcription (RT^2-PCR) analysis were used to validate microarray data using a set of genes selected because of their significant fold-change expression differences at 6h and/or 12h. First strand cDNA was prepared from 100 ng total RNA following the protocol for the SuperScript II First Strand cDNA Synthesis system (Invitrogen, Carlsbad, CA). After selecting a panel of genes of interest (**Supplemental Table 1**), RT^2-PCR was performed using protocols provided by the commercial provider of primers and master mix (SA Biosciences, Frederick, MD) in an iCycler System (Biorad, Hercules, CA). Fold-changes in expression of genes from TCDD-treated LSK were calculated with respect to vehicle-treated LSK using the $2^{-\Delta\Delta Ct}$ approximation method. *Gapdh* and *Hprt1* were used as control endogenous genes to normalize gene expression. A linear regression coefficient close to one was used to assess validation of microarray data with RT^2-PCR.

Gene Expression Analysis

Transcripts with a fold-change expression (TCDD normalized expression/Vehicle normalized expression) greater than 1.5 at each time-point were filtered. The most variable transcripts were visualized using the open-source software TIGR Multi-experiment Viewer (MeV) (version 4.6.1) (Saeed, et al., 2003). Relevant Functional Association Networks were generated by Ingenuity Pathway Analysis (IPA) Software (version 8.7) (Ingenuity Systems, Redwood City, CA). For this purpose, the data sets containing all gene identifiers and corresponding fold-change expression values were up-loaded into the application. Each identifier was mapped to its corresponding

Downloaded from molpharm.aspetjournals.org at ASPET Journals on April 17, 2024

Molecular Pharmacology Fast Forward. Published on July 26, 2011 as DOI: 10.1124/mol.111.071381
This article has not been copyedited and formatted. The final version may differ from this version.

object in Ingenuity's Knowledge Base. A 1.5 cut-off of fold-change was set to identify transcripts whose expression was regulated. Transcripts with altered expression were overlaid onto a global molecular network developed from information contained in Ingenuity's Knowledge Base.

Statistical Analyses

Unless otherwise specified, results were analyzed and plotted using GraphPad Prism (version 5.03) (GraphPad Software, Inc, La Jolla, CA). The p-value of Pearson's Chi-square test for goodness of fit to a binomial distribution (p=1) was used to analyze the CRU data. When appropriate, two-tailed Student's T-test and two-way ANOVA were used to analyze statistical significance. P-values smaller than 0.05 were considered to be statistically significant *$p<0.05$, **$p<0.001$, and ***$p<0.0001$. Right-tailed Fisher's exact test was used to calculate a p-value determining the probability that each biological function and/or disease assigned to that data set by IPA is due to chance alone.

Downloaded from molpharm.aspetjournals.org at ASPET Journals on April 17, 2024

Molecular Pharmacology Fast Forward. Published on July 26, 2011 as DOI: 10.1124/mol.111.071381
This article has not been copyedited and formatted. The final version may differ from this version.

Results

AhR activation by TCDD alters phenotype and functions of HSCs

Our laboratory and others have consistently observed alterations of phenotypically-defined HSCs/progenitors after TCDD treatment (Murante and Gasiewicz, 2000; Sakai, et al., 2003; Singh, et al., 2009). In this study, we asked questions about the relative expression of newly recognized phenotypes of HSCs (Kiel, et al., 2005) as well as qualitative and quantitative functional characteristics of BM cells. Seven days after *in vivo* treatment with TCDD, populations of HSCs were analyzed using flow cytometry based on their relative expression of the Signaling Lymphocyte Activation Molecule (SLAM) receptors (Wilson, et al., 2008) as phenotypic markers of BM stem cells. **Figure 1A** shows representative gating applied to all samples used to determine the relative percentages of LSK, LSKCD48$^-$CD150$^-$ and LSKCD48$^-$CD150$^+$ populations. As observed previously (Murante and Gasiewicz, 2000; Singh, et al., 2009), TCDD treatment resulted in a significant increase in the relative percentage of LSK cells (**Fig. 1B**). However, only a small proportion of the LSK population is made up of those cells defined as HSCs, with the largest sub-population being composed of predominantly more mature multi-potent progenitor (MPP) cells. As such, it is notable that TCDD also increased the relative percentages of the sub-populations LSKCD48$^-$CD150$^-$ and LSKCD48$^-$CD150$^+$ which have been correlated with short-term HSCs and MPPs, and long-term HSCs, respectively (**Fig. 1C**).

To characterize the functional quality of HSCs, the progeny of short-term and long-term HSC donor cells was analyzed after 6 or 20 weeks of competitive repopulation, respectively. Hematopoietic cells from a donor or competitive donor origin were distinguished using flow cytometry (**Figs. 2A-C**). Under the experimental conditions used, no differences between TCDD and vehicle were observed 6 (**Fig. 2D**) or 20 (**Fig. 2E**) weeks post-transplantation. The proportions of short- and long-term HSCs per million BM cells (**Table 1**) were calculated from

Downloaded from molpharm.aspetjournals.org at ASPET Journals on April 17, 2024

Molecular Pharmacology Fast Forward. Published on July 26, 2011 as DOI: 10.1124/mol.111.071381
This article has not been copyedited and formatted. The final version may differ from this version.

limiting dilution analysis to characterize quantitatively the functional integrity of these cells. By this analysis, the numbers of competitive functional HSCs from TCDD-treated animals were not significantly different from vehicle controls. To complement this analysis, we evaluated the ability of LSK cells from TCDD-treated mice to undergo expansion and differentiation under *ex vivo* conditions. **Supplemental Figure 1** shows that, in the presence of IL-6 ± stem cell factor (Scf), TCDD-treated LSKs are as able to grow and generate different Lin^- and Lin^+ populations *in vitro* similarly as vehicle-treated LSKs. Also, LSKs from TCDD-treated mice didn't show any difference in the level of apoptosis as measured by Annexin and 7AAD staining (**Supplemental Figure 2**). These results suggested that the TCDD dosing paradigm used to activate the AhR elicited phenotypic changes, but did not alter the absolute proportions of functional HSCs when measured independently from their correlated phenotype. Also, there were no alterations of their ability to survive, expand and differentiate under *ex vivo* conditions.

TCDD affects migration of LSKs

TCDD-treated LSK cells were reported to have a decreased engraftment (Sakai, et al. 2003; Singh, et al. 2009). However, TCDD treatment elicited no difference in the overall proportions of functional HSCs independently from their phenotype (**Table 1**). Therefore, we hypothesized that critical events during engraftment such as trafficking behavior of LSKs may be affected. **Figure 3A** shows that migration of LSK cells from TCDD-treated animals to BM of recipients is decreased when measured as *in vivo* accumulation of cells to the BM after 24 hours of transplantation. As a complement to this study, we also observed that the directional migration of TCDD-treated LSK cells through a semi-permeable membrane to a chamber containing the chemokine CXCL12 was decreased (**Fig. 3B**).

The best studied receptor of CXCL12 is CD184 (CXCR4) (Sasaki, et al., 2009). As such, we analyzed LSK cells for the expression of CD184/CXCR4 as well as other molecules known to

Downloaded from molpharm.aspetjournals.org at ASPET Journals on April 17, 2024

Molecular Pharmacology Fast Forward. Published on July 26, 2011 as DOI: 10.1124/mol.111.071381
This article has not been copyedited and formatted. The final version may differ from this version.

participate in the interactions between HSCs and their microenvironment such as CD44 which is a receptor for osteopontin present in the extra-cellular matrix of the endosteum. Within the LSK population from TCDD-treated animals, there was increased Mean Fluorescent Intensity for CD184/CXCR4 and CD44 (**Figs. 3C and 3D**). Together these results support that AhR activation leads to cell signaling-mediated disruptions in the ability of LSKs to interact with molecules present in their microenvironment.

TCDD alters pathways involved in cell signaling, cellular movement and cancer.

The above data suggest that the previously observed TCDD-elicited changes in HSC/progenitor engraftment (Sakai, et al., 2003; Singh, et al., 2009) were due predominantly, if not exclusively, to altered homing of HSCs from TCDD-treated animals. Alterations in the expression and/or function of CD184/CXCR4 and CD44 on these cells are likely concomitant with functional changes. Being that the AhR is a transcription factor, we hypothesized that the phenotypic and cellular changes observed above were the consequence of AhR-mediated changes in gene expression. Differential gene expression in LSKs from mice treated with TCDD (30 μg/kg) or vehicle for 6h and 12h was analyzed using microarray technology. Hierarchical clustering of the expression profiles showed that the most significant changes in regulation occurred for 105 transcripts (**Fig. 4A**). Transcripts consistently up-regulated at 6h and 12h included Scinderin (*Scin*), *Mmp8,* Interleukin 1 family member 9 (*Il1f9*), NAD(P)H dehydrogenase quinone 1 (*Nqo1*), Filamin beta (*Flnb*), mouse predicted gene *Gm5662*, and SLAM family member 7 (*Slamf7*) (**Table 2**). The lists of up- or down-regulated transcripts at 6h and 12h can be found in **Supplemental Tables 2, 3,** and **4**. Results from RT^2-PCR analyses, (**Figs. 4B** and **4C)** validate the changes observed at 6h and 12h. There were some notable differences between the responses at 6 and 12 h. At 6 h, several genes (*Olfr1095, Mmp9, Ceacam10, Retnig, Msr1, and Lcn2*) were up-regulated > two-fold, but demonstrated no significant change at 12 h (**Fig. 4A**, **Table S2**). In contrast, other genes including *Fosb, Cxcl2, Egr1, Atf3, Nr4a1, Fos, Jun,*

Downloaded from molpharm.aspetjournals.org at ASPET Journals on April 17, 2024

Molecular Pharmacology Fast Forward. Published on July 26, 2011 as DOI: 10.1124/mol.111.071381
This article has not been copyedited and formatted. The final version may differ from this version.

Junb, Dusp1, Plk2, Ptgs2 (Cox2), Cd69, Ighg, Slc10a1, and *Myd116*, were down-regulated at 6 h, but were significantly up-regulated (*Cxcl2, Nr4a1, Plk2, Ptgs2, Cd69*) or not altered at 12 h (**Fig. 4A**,**Tables S3 and S4**).

In order to understand the biological relevance of the observed changes, IPA was used to generate Functional Association Networks with the following settings: direct relationships from the Ingenuity Knowledge Base Reference Set reported in all human, mouse and rat immune primary cells; and immune, leukemia, lymphoma, macrophage and myeloma cell lines; cut-off fold-changes values 1.5; up to 25 networks per analysis; up to 35 molecules per network. **Table 3** shows that the common top biological functions at 6h and 12h were cell-to-cell signaling and interaction, and cellular movement. Also, at these time-points, hematological system development and function was significantly affected by treatment. **Supplemental Tables 5 and 6** show the detailed lists of transcripts assigned by IPA to the most relevant molecular and cellular functions, and physiological systems and functions. Notably, changes in genes involved in the biological functions of antigen presentation, cell-to-cell signaling and interaction, cellular movement, hematological system development and function, and immune cell trafficking appeared to be most significant (defined by p-values < 10^{-7}) in the 12h response to TCDD (**Table 3**). **Figure 5** shows functional association networks of transcripts assigned to hematological system development and function, generated by IPA at 6h and 12h. An analysis was also run using information reported from hematopoietic and non-hematopoietic cells. According to this analysis, the top biological functions and diseases associated with the network generated by the molecular interactions common to both time-points were gene expression (*RNA polymerase II, histone h3, histone h4*), inflammation (*Ptgs2* also known as *Cox2, NFκB complex*), and cancer (*Ptgs2*, *Cxcl2*, *Jun, Fos, Atf3, Mmp9, Nqo1, Nr4a1, Cd69, Btg2, Egr1, Dusp1*).

Downloaded from molpharm.aspetjournals.org at ASPET Journals on April 17, 2024

Molecular Pharmacology Fast Forward. Published on July 26, 2011 as DOI: 10.1124/mol.111.071381
This article has not been copyedited and formatted. The final version may differ from this version.

Discussion

There is increasing evidence supporting a role of the AhR in hematopoiesis, and HSC biology in particular. In part, this evidence comes from reports of increased incidence of leukemia and non-Hodgkin's lymphoma in TCDD-exposed populations (Frumkin 2003), as well as recent studies suggesting a potential therapeutic application of AhR antagonists to expand human HSCs for BM transplants (Boitano, et al., 2010). As such, there is a need to define cellular and molecular mechanisms whereby the AhR mediates these effects.

It has been shown that TCDD exposure to mice increases the percentages of LSKs, and some LSK sub-populations in BM (Sakai, et al., 2003; Singh, et al., 2009). Here we expand on these reports by showing that the percentage of LSKCD48$^-$CD150$^-$ and LSKCD48$^-$CD150$^+$ stem cells, identified by the recently described SLAM markers (Kiel, et al. 2005), are also increased following TCDD treatment (**Fig. 1**). These results present the apparent paradox that higher percentages of phenotypically-defined HSCs (LSKs) occurred with a decreased functional ability of these cells to generate progeny (Sakai, et al. 2003; Singh, et al. 2009). This may not necessarily be contradictory since it has been reported that when homeostasis is disrupted, cells with the phenotype of HSCs may have an altered functional capacity (Purton and Scadden, 2007). To avoid potential biases inherent with phenotypic-based sorting and defined relative ratios of donor to competitor cell numbers, we used a limiting dilution approach to quantify the functional integrity of these cells. These studies indicated no significant differences in the absolute proportions of LT- and ST-HSCs from TCDD- and vehicle-treated mice (**Table 1**). Together, these data suggested that the higher percentages of phenotypically-defined HSCs reflected changes in HSC biology and cell signaling that may affect different steps of the engraftment process.

Successful engraftment of HSCs involves a number of different events such as leaving the

Downloaded from molpharm.aspetjournals.org at ASPET Journals on April 17, 2024

Molecular Pharmacology Fast Forward. Published on July 26, 2011 as DOI: 10.1124/mol.111.071381
This article has not been copyedited and formatted. The final version may differ from this version.

circulation to home to the BM, taking residence in the vascular and endosteal niches, and finally lineage differentiation. Our studies further demonstrated that TCDD-mediated activation of the AhR alters the migration and trafficking of phenotypically-defined HSCs under *in vivo* and *in vitro* conditions (**Figs. 3A and 3B**). Thus, previously observed decreased engraftment (Sakai, et al. 2003; Singh, et al. 2009) is likely due to decreased migration (**Figure 3**) rather than decreased numbers of functional HSCs (**Fig. 2 and Table 1**) or altered viability and differentiation (**Supplemental Figs. 1 and 2**). A modified ability of HSCs and progenitors to move within the marrow niche may also explain the effects of AhR activation by TCDD on more differentiated cells i.e. decreased thymic seeding (Fine, et al., 1990; Laiosa, et al., 2010), and altered B cell numbers (Thurmond, et al., 2000).

Trafficking events are dependent on the ability of HSCs to "sense" their microenvironment by cell-cell interactions and the recognition of soluble factors through cell surface proteins. Markers used for phenotypic discrimination are functional molecules themselves involved in cell signaling through recognition of chemical cues from the microenvironment to migrate, differentiate, proliferate, or self-renew. For example, c-kit is a tyrosine kinase serving as a receptor of the stem cell factor, which provides cues for quiescence and survival of the most primitive progenitor cells in the BM (Askmyr, et al., 2009). CD184/CXCR4 is critical during development for seeding of the BM with HSCs, and mediates migration and quiescence throughout adulthood (Nie, et al., 2008). CD44 is highly expressed in pro-thymocytes ($CD4^{low}CD25^{-}c\text{-}kit^{+}$) of the BM serving as a homing receptor for the thymus (Wu, et al., 1993), and CD44 expression was found to be up-regulated in thymic emigrants exposed to TCDD (Esser, et al. 2004). As such, it is reasonable, if not expected, that functional alterations in HSCs following TCDD treatment would be a reflection of altered expression and/or function of cell surface proteins. However, we observed an increase, rather than an expected decreased, phenotypic expression of both CD184/CXCR4 and CD44 at 7 d following TCDD treatment (**Fig. 3**). No differences were

Downloaded from molpharm.aspetjournals.org at ASPET Journals on April 17, 2024

Molecular Pharmacology Fast Forward. Published on July 26, 2011 as DOI: 10.1124/mol.111.071381
This article has not been copyedited and formatted. The final version may differ from this version.

observed in CD184/CXCR4 or CD44 mRNA expression at 6 or 12h post TCDD exposure as determined by the microarray data. Also, CD184/CXCR4 mRNA expression at 24h or 7d following TCDD exposure was not changed as determined by RT^2-PCR analysis (not shown). Together these data suggest that TCDD may cause altered CD184/CXCR4 and CD44 protein expression in HSCs by a post-transcriptional mechanism, and that other molecules are being affected by AhR activation that either alter the function of these proteins or that are involved the migration and trafficking of these cells.

Given that the AhR is a ligand-activated transcription factor, we hypothesize that TCDD-mediated changes in phenotype and signaling of HSCs were preceded by changes in gene expression. The results shown in **Figures 4** and **5** support this hypothesis. Multiple transcriptional changes occurred 6h after exposure, some of which were transient and other were also observed 6h later. The genes modulated by AhR activation in LSKs that have been reported to have putative AhREs (Sun, et al., 2004) in the promoters of their murine homologs include *Scin, Nqo1, Egr1, Ptgs2, Cxcl2, Nr4a1, Dusp1, Btg2, Junb, Fosb, Jun, Ceacam10, Scrg1, C1qb, Bst1, Slc10a1, Spp1, Snord14a, Ier2, Ccl4, Skil, and Klrb1c*, although it is not yet clear whether all of these sites represent AhREs that are functional.

Scinderin (*Scin*, also known as adseverin) was highly up-regulated both after 6h and 12 h of TCDD-treatment (**Table 2**). In hematopoietic stem and progenitor cells, *Scin* is one of the key regulators accounting for chemotactic responses to CXCL12 (Evans, et al., 2004). This calcium/proton-regulated protein binds actin monomers, severs and caps actin filaments, and has been reported to respond to TCDD treatment in other immune cells (Svensson, et al., 2002). Sequential coordinated polymerization and depolymerization of the actin cytoskeleton is necessary to maintain the functional expression of cell surface proteins and for directed migration (Friederich, et al., 1992). CD184/CXCR4 function and cell surface expression is known to depend on endocytosis, intracellular trafficking and recycling (Kumar, Kremer et al.

Downloaded from molpharm.aspetjournals.org at ASPET Journals on April 17, 2024

Molecular Pharmacology Fast Forward. Published on July 26, 2011 as DOI: 10.1124/mol.111.071381
This article has not been copyedited and formatted. The final version may differ from this version.

2011), all of which are dependent on cytoskeleton regulation. $Lin^{-}Sca\text{-}1^{+}ckit^{-}$ and LSKs move with different efficiencies towards CXCL12 due at least in part to different expression of Scin protein (Evans, et al., 2004). Given that TCDD can regulate *Scin* transcripts and responses to CXCL12 in LSKs, our results support a role for the AhR in cytoskeleton regulation that may have consequences for cell motility.

Mmp8 was also up-regulated at both time points. Even though there is no evidence of AhR transcriptionally regulating metalloproteinases, there is literature linking AhR activation with their expression, probably via *Jun* or *Fos* (Hillegass, et al., 2006). Together with CD184, metalloproteinases have been proposed to be involved in cell migration and invasion of leukemic cells (Shao, et al., 2011). Different transcripts involved in NFκB signaling such as *Il1f9, Cxcl2, Ptgs2, Junb,* and *Fos* (**Table 2 and Supplemental Table 3**) were also altered at both time-points. Whether these changes in gene expression are directly related to AhR-DNA binding in LSKs is uncertain since there is evidence that AhR and NFκB proteins can interact directly (Tian, 2009). Further kinetic studies to clarify these interactions are of therapeutic interest considering that NFκB complexes regulate CD184 (Chua, et al., 2010) and CD44 (Damm, et al., 2010) protein expression. It is also of interest that *Spp1* was down-regulated 6h after TCDD-exposure. *Spp1* encodes osteopontin, one of the ligands of CD44. The reduced expression of a CD44 ligand (**Supplemental Table 4**) at early time-points may be related with increased CD44 expression (**Fig. 3C**) several days later. Given that some of the transcripts changed in our data sets are themselves transcriptional regulators and are regulated by the AhR (e.g. *Fos*, *JunB, Ptgs2, Egr1)*, it seems likely that some of the functional changes are secondary to initial AhR signaling. While supporting the functional changes that we observed in hematopoietic stem/progenitor cells after TCDD treatment, the changes in gene expression also suggest a complex crosstalk of the AhR with pathways associated with the ability of HSCs to sense their microenvironment, alter their trafficking behavior, and promote hematological diseases, which is

Downloaded from molpharm.aspetjournals.org at ASPET Journals on April 17, 2024

Molecular Pharmacology Fast Forward. Published on July 26, 2011 as DOI: 10.1124/mol.111.071381
This article has not been copyedited and formatted. The final version may differ from this version.

a common sequence of events in leukemogenesis.

Together, these results suggest a complex role of AhR signaling in HSC function. Additional studies in *AhR* null mice suggest that AhR may regulate HSC quiescence/proliferation (Singh, et al., 2010) that, consistent with the present study, depend on the ability of HSCs to sense cues within their microenvironment. It is also important to consider that the exact role of the AhR and its physiological relevance in other tissue stem cell populations may be context-specific (Latchney, et al., 2010; Panteleyev and Bickers, 2006). Clinical use of the AhR to treat hematological diseases (Boitano, et al., 2010; Quintana, et al., 2010) will also require answering daunting questions regarding the biological implications of different, and possibly endogenous, ligands in AhR activity and the relevance of non-genomic pathways in AhR signaling. Nevertheless, further investigations in this area will provide important information needed for our understanding of processes that regulate stem cells and their role in human disease.

Downloaded from molpharm.aspetjournals.org at ASPET Journals on April 17, 2024

Molecular Pharmacology Fast Forward. Published on July 26, 2011 as DOI: 10.1124/mol.111.071381
This article has not been copyedited and formatted. The final version may differ from this version.

Acknowledgements

We thank Dr. Ellen Henry for critical discussion and reading of the manuscript, Jason Walrath for assistance with animal care, Dr. Timothy Bushnell and the staff of the Flow Core Facilities in URMC, and Dr. Stephen Welle and the staff of the Functional Genomics Core of the URMC.

Downloaded from molpharm.aspetjournals.org at ASPET Journals on April 17, 2024

Molecular Pharmacology Fast Forward. Published on July 26, 2011 as DOI: 10.1124/mol.111.071381
This article has not been copyedited and formatted. The final version may differ from this version.

Authorship contributions

Participated in research design: Casado, Singh and Gasiewicz

Conducted experiments: Casado and Singh

Performed data analysis: Casado, Singh, Gasiewicz,

Wrote or contributed to the writing of this manuscript: Casado, Gasiewicz and Singh

Downloaded from molpharm.aspetjournals.org at ASPET Journals on April 17, 2024

Molecular Pharmacology Fast Forward. Published on July 26, 2011 as DOI: 10.1124/mol.111.071381
This article has not been copyedited and formatted. The final version may differ from this version.

References

Askmyr M, Sims NA, Martin TJ and Purton LE (2009) What is the true nature of the osteoblastic hematopoietic stem cell niche? *Trends Endocrinol Metab* 20:303-309.

Boitano AE, Wang J, Romeo R, Bouchez LC, Parker AE, Sutton SE, Walker JR, Flaveny CA, Perdew GH, Denison MS, Schultz PG and Cooke MP (2010) Aryl hydrocarbon receptor antagonists promote the expansion of human hematopoietic stem cells. *Science* 329:1345-1348.

Chua AW, Hay HS, Rajendran P, Shanmugam MK, Li F, Bist P, Koay ES, Lim LH, Kumar AP and Sethi G (2010) Butein downregulates chemokine receptor CXCR4 expression and function through suppression of NF-kappaB activation in breast and pancreatic tumor cells. *Biochem Pharmacol* 80:1553-1562.

Damm S, Koefinger P, Stefan M, Wels C, Mehes G, Richtig E, Kerl H, Otte M and Schaider H (2010) HGF-promoted motility in primary human melanocytes depends on CD44v6 regulated via NF-kappa B, Egr-1, and C/EBP-beta. *J Invest Dermatol* 130:1893-1903.

Esser C, Temchura V, Majora M, Hundeiker C, Schwarzler C and Gunthert U (2004) Signaling via the AHR leads to enhanced usage of CD44v10 by murine fetal thymic emigrants: possible role for CD44 in emigration. *Int Immunopharmacol* 4:805-818.

Evans CA, Tonge R, Blinco D, Pierce A, Shaw J, Lu Y, Hamzah HG, Gray A, Downes CP, Gaskell SJ, Spooncer E and Whetton AD (2004) Comparative proteomics of primitive hematopoietic cell populations reveals differences in expression of proteins regulating motility. *Blood* 103:3751-3759.

Downloaded from molpharm.aspetjournals.org at ASPET Journals on April 17, 2024

Molecular Pharmacology Fast Forward. Published on July 26, 2011 as DOI: 10.1124/mol.111.071381
This article has not been copyedited and formatted. The final version may differ from this version.

Fine JS, Silverstone AE and Gasiewicz TA (1990) Impairment of prothymocyte activity by 2,3,7,8-tetrachlorodibenzo-p-dioxin. *J Immunol* 144:1169-1176.

Frericks M, Meissner M and Esser C (2007) Microarray analysis of the AHR system: tissue-specific flexibility in signal and target genes. *Toxicol Appl Pharmacol* 220:320-332.

Friederich E, Vancompernolle K, Huet C, Goethals M, Finidori J, Vandekerckhove J and Louvard D (1992) An actin-binding site containing a conserved motif of charged amino acid residues is essential for the morphogenic effect of villin. *Cell* 70:81-92.

Frumkin H (2003) Agent Orange and cancer: an overview for clinicians. *CA Cancer J Clin* 53:245-255.

Henry EC, Welle SL and Gasiewicz TA (2010) TCDD and a putative endogenous AhR ligand, ITE, elicit the same immediate changes in gene expression in mouse lung fibroblasts. *Toxicol Sci* 114:90-100.

Hillegass JM, Murphy KA, Villano CM and White LA (2006) The impact of aryl hydrocarbon receptor signaling on matrix metabolism: implications for development and disease. *Biol Chem* 387:1159-1173.

Kiel MJ, Yilmaz OH, Iwashita T, Yilmaz OH, Terhorst C and Morrison SJ (2005) SLAM family receptors distinguish hematopoietic stem and progenitor cells and reveal endothelial niches for stem cells. *Cell* 121:1109-1121.

Kremer J, Gleichmann E and Esser C (1994) Thymic stroma exposed to arylhydrocarbon receptor-binding xenobiotics fails to support proliferation of early thymocytes but induces differentiation. *J Immunol* 153:2778-2786.

Downloaded from molpharm.aspetjournals.org at ASPET Journals on April 17, 2024

Molecular Pharmacology Fast Forward. Published on July 26, 2011 as DOI: 10.1124/mol.111.071381
This article has not been copyedited and formatted. The final version may differ from this version.

Kumar A, Kremer KN, Dominguez D, Tadi M and Hedin KE (2011) Galpha13 and Rho mediate endosomal trafficking of CXCR4 into Rab11+ vesicles upon stromal cell-derived factor-1 stimulation. *J Immunol* 186:951-958.

Laiosa MD, Mills JH, Lai ZW, Singh KP, Middleton FA, Gasiewicz TA and Silverstone AE (2010) Identification of stage-specific gene modulation during early thymocyte development by whole-genome profiling analysis after aryl hydrocarbon receptor activation. *Mol Pharmacol* 77:773-783.

Latchney SE, Lioy DT, Henry EC, Gasiewicz TA, Strathmann FG, Mayer-Proschel M and Opanashuk LA (2010) Neural Precursor Cell Proliferation Is Disrupted Through Activation of the Aryl Hydrocarbon Receptor by 2,3,7,8-Tetrachlorodibenzo-p-Dioxin. *Stem Cells Dev* 20:313-326.

Murante FG and Gasiewicz TA (2000) Hemopoietic progenitor cells are sensitive targets of 2,3,7,8-tetrachlorodibenzo-p-dioxin in C57BL/6J mice. *Toxicol Sci* 54:374-383.

Mustafa A, Holladay SD, Goff M, Witonsky SG, Kerr R, Reilly CM, Sponenberg DP and Gogal RM,Jr (2008) An enhanced postnatal autoimmune profile in 24 week-old C57BL/6 mice developmentally exposed to TCDD. *Toxicol Appl Pharmacol* 232:51-59.

Nie Y, Han YC and Zou YR (2008) CXCR4 is required for the quiescence of primitive hematopoietic cells. *J Exp Med* 205:777-783.

Poland A and Glover E (1973) Studies on the mechanism of toxicity of the chlorinated dibenzo-p-dioxins. *Environ Health Perspect* 5:245-251.

Purton LE and Scadden DT (2007) Limiting factors in murine hematopoietic stem cell assays. *Cell Stem Cell* 1:263-270.

Downloaded from molpharm.aspetjournals.org at ASPET Journals on April 17, 2024

Molecular Pharmacology Fast Forward. Published on July 26, 2011 as DOI: 10.1124/mol.111.071381
This article has not been copyedited and formatted. The final version may differ from this version.

Quintana FJ, Murugaiyan G, Farez MF, Mitsdoerffer M, Tukpah AM, Burns EJ and Weiner HL (2010) An endogenous aryl hydrocarbon receptor ligand acts on dendritic cells and T cells to suppress experimental autoimmune encephalomyelitis. *Proc Natl Acad Sci U S A* 107:20768-20773.

Saeed AI, Sharov V, White J, Li J, Liang W, Bhagabati N, Braisted J, Klapa M, Currier T, Thiagarajan M, Sturn A, Snuffin M, Rezantsev A, Popov D, Ryltsov A, Kostukovich E, Borisovsky I, Liu Z, Vinsavich A, Trush V and Quackenbush J (2003) TM4: a free, open-source system for microarray data management and analysis. *BioTechniques* 34:374-378.

Sakai R, Kajiume T, Inoue H, Kanno R, Miyazaki M, Ninomiya Y and Kanno M (2003) TCDD treatment eliminates the long-term reconstitution activity of hematopoietic stem cells. *Toxicol Sci* 72:84-91.

Sasaki Y, Matsuoka Y, Hase M, Toyohara T, Murakami M, Takahashi M, Nakatsuka R, Uemura Y and Sonoda Y (2009) Marginal expression of CXCR4 on c-kit(+)Sca-1 (+)Lineage (-) hematopoietic stem/progenitor cells. *Int J Hematol* 90:553-560.

Shao HY, Miao ZY, Hui-Chen, Qin FX, Chen XC, Tan S, Zhang HJ, Wang L, Gao YJ, Yang ZL and Zhang L (2011) Nucleophosmin gene mutations promote NIH3T3 cell migration and invasion through CXCR4 and MMPs. *Exp Mol Pathol* 90:38-44.

Singh KP, Garrett RW, Casado FL and Gasiewicz TA (2010) Aryl hydrocarbon receptor-null allele mice have abnormal characteristics and functions of hematopoietic stem/progenitor cells. *Stem Cells Dev* 20:769-784.

Downloaded from molpharm.aspetjournals.org at ASPET Journals on April 17, 2024

Molecular Pharmacology Fast Forward. Published on July 26, 2011 as DOI: 10.1124/mol.111.071381
This article has not been copyedited and formatted. The final version may differ from this version.

Singh KP, Wyman A, Casado FL, Garrett RW and Gasiewicz TA (2009) Treatment of mice with the Ah receptor agonist and human carcinogen dioxin results in altered numbers and function of hematopoietic stem cells. *Carcinogenesis* 30:11-19.

Soshilov A and Denison MS (2008) Role of the Per/Arnt/Sim domains in ligand-dependent transformation of the aryl hydrocarbon receptor. *J Biol Chem* 283:32995-33005.

Staples JE, Murante FG, Fiore NC, Gasiewicz TA and Silverstone AE (1998) Thymic alterations induced by 2,3,7,8-tetrachlorodibenzo-p-dioxin are strictly dependent on aryl hydrocarbon receptor activation in hemopoietic cells. *J Immunol* 160:3844-3854.

Stevens EA, Mezrich JD and Bradfield CA (2009) The aryl hydrocarbon receptor: a perspective on potential roles in the immune system. *Immunology* 127:299-311.

Sun YV, Boverhof DR, Burgoon LD, Fielden MR and Zacharewski TR (2004) Comparative analysis of dioxin response elements in human, mouse and rat genomic sequences. *Nucleic Acids Res* 32:4512-4523.

Svensson C, Silverstone AE, Lai ZW and Lundberg K (2002) Dioxin-induced adseverin expression in the mouse thymus is strictly regulated and dependent on the aryl hydrocarbon receptor. *Biochem Biophys Res Commun* 291:1194-1200.

Thurmond TS, Staples JE, Silverstone AE, Gasiewicz TA (2000) The aryl hydrocarbon receptor has a role in the in vivo maturation of murine bone marrow B lymphocytes and their response to 2,3,7,8-tetrachlorodibenzo-p-dioxin. Toxicol Appl Pharmacol 165:227-236.

Tian Y (2009) Ah receptor and NF-kappaB interplay on the stage of epigenome. *Biochem Pharmacol* 77:670-680.

Downloaded from molpharm.aspetjournals.org at ASPET Journals on April 17, 2024

Molecular Pharmacology Fast Forward. Published on July 26, 2011 as DOI: 10.1124/mol.111.071381
This article has not been copyedited and formatted. The final version may differ from this version.

Wilson A, Laurenti E, Oser G, van der Wath RC, Blanco-Bose W, Jaworski M, Offner S, Dunant CF, Eshkind L, Bockamp E, Lio P, Macdonald HR and Trumpp A (2008) Hematopoietic stem cells reversibly switch from dormancy to self-renewal during homeostasis and repair. *Cell* 135:1118-1129.

Wu L, Kincade PW and Shortman K (1993) The CD44 expressed on the earliest intrathymic precursor population functions as a thymus homing molecule but does not bind to hyaluronate. *Immunol Lett* 38:69-75.

Downloaded from molpharm.aspetjournals.org at ASPET Journals on April 17, 2024

Molecular Pharmacology Fast Forward. Published on July 26, 2011 as DOI: 10.1124/mol.111.071381
This article has not been copyedited and formatted. The final version may differ from this version.

Footnotes

- This work was funded by the National Institutes of Health Center Grant [ES01247], Training Grant [ES07026], and Research Grants [ES04862 and ES016606].
- Corresponding author: Dr. Thomas A. Gasiewicz, Department of Environmental Medicine, University of Rochester School of Medicine, Box-EHSC, 601. Elmwood Avenue, Rochester, NY 14642. Phone: (585) 275-3265, Fax: (585) 256-2591. Email: **Tom_Gasiewicz@urmc.rochester.edu**

Downloaded from molpharm.aspetjournals.org at ASPET Journals on April 17, 2024

Molecular Pharmacology Fast Forward. Published on July 26, 2011 as DOI: 10.1124/mol.111.071381
This article has not been copyedited and formatted. The final version may differ from this version.

Legends for figures

Figure 1. TCDD treatment altered phenotypically-defined HSC populations.

Lin^- cells were harvested from mice treated with TCDD (30 μg/kg, 7d) or vehicle. Flow cytometry was used to phenotypically characterize populations of HSCs. (A) Dead cells were excluded and the LSK population was gated from the viable cells. From the LSK population, further gating was applied based on CD48 and CD150. Cumulative data for the percentages of the HSC-enriched population are indicated. (B) LSK (p-value = 0.0059), and sub-populations (C) $LSKCD48^-CD150^-$ (p-value = 0.0075) and $LSKCD48^-CD150^+$ (p-value = 0.0007) in Lin^- cells. Error bars are S.E.M. for n=3 independent experiments using data from 5-6 individual mice.

Figure 2. Qualitative analysis of engrafted TCDD–treated BM cells shows no difference in the engraftment potential of HSCs.

Donor $CD45.2^+$ BM cells from TCDD-treated (30 μg/kg, 7d) mice were simultaneously injected with $CD45.1^+$ competitor BM cells at different ratios into $CD45.1^+$ irradiated recipient mice. Representative gating applied for (A) competitive donor BM cells and (B) donor BM cells. After reconstitution, the long-term (20 weeks) and short-term (6 weeks) ability to reconstitute the BM was qualitatively analyzed. (C) Flow cytometry was used to discriminate $CD45.2^+$ donor cells from $CD45.1^+$ competitive donor cells in repopulated recipients. Cumulative data for the percentage of donor's progeny ($CD45.2^+$) show no differences (D) 6 or (E) 20 weeks post-transplantation. Data shown represent one independent experiment of two with eight recipients per group per experiment. Squares represent values for individual mice. Average values for vehicle and TCDD groups are represented by dashed and solid lines, respectively.

Figure 3. TCDD exposure altered the migration of HSCs *in vivo* and *in vitro*.

Downloaded from molpharm.aspetjournals.org at ASPET Journals on April 17, 2024

Molecular Pharmacology Fast Forward. Published on July 26, 2011 as DOI: 10.1124/mol.111.071381
This article has not been copyedited and formatted. The final version may differ from this version.

BM cells were harvested from mice treated with TCDD (30 μg/kg, 7d) or vehicle. (A) Five million $CD45.2^+$ BM cells from TCDD-treated or untreated mice were injected intravenously into $CD45.1^+$ recipients. After 24 h, flow cytometry was used to determine the numbers of donor LSKs that migrated to BM in recipients with respect to the LSK numbers injected. (p-value = 0.0242). Error bars are S.E.M of n=3 independent experiments using data from 5-6 individual mice per experiment. (B) Half a million Lin^- cells were placed on top of a transwell migration chamber containing 50-300 ng/mL of CXCL12 in the bottom chamber. Three hours later, LSK cells that migrated to the bottom chamber were counted by flow cytometry. Two-way ANOVA analysis indicated significant differences at 100 and 300 ng/mL (p-values < 0.0001). Error bars are S.E.M. of n=3 independent experiments using data from 12 wells with cells from three pooled mice. (C) LSK cells were analyzed for expression of surface molecules by flow cytometry. Two-way ANOVA analysis indicated significant differences between groups for CD184/CXCR4 and CD44 (p-values = 0.0037 and <0.0001, respectively). Error bars are S.E.M. of n=3 independent experiments using data from 5-6 individual mice. (D) Representative histograms obtained using flow cytometry to determine the Mean Fluorescent Intensity of CD184/CXCR4 and CD44 in viable LSK cells. The filled histograms are representative of TCDD– (black) and vehicle-treated cells (grey). Unfilled histograms are representative of the negative controls used to compensate fluorescent signals, that were stained with all of the fluorochromes used in the respective panels except with the one conjugated to the protein being analyzed (CD184 or CD44). The horizontal bars represent the gating used to determine the positive population of cells where the Mean Fluorescent Intensity was calculated.

Figure 4. TCDD exposure induced changes in the expression of genes in LSK cells.

Total RNA was obtained from sorted LSK cells. Fold-changes in normalized values of gene expression for TCDD or vehicle control groups were calculated using microarray technology. Microarray data represent averages of five experiments using RNA from LSKs pooled from 20

Downloaded from molpharm.aspetjournals.org at ASPET Journals on April 17, 2024

Molecular Pharmacology Fast Forward. Published on July 26, 2011 as DOI: 10.1124/mol.111.071381
This article has not been copyedited and formatted. The final version may differ from this version.

mice per treatment. (A) The most variable transcripts from the 6h and 12h datasets (Fold-change > 1.5) were visualized using MeV. The intensity of the colors represents the changes in fold-change for the up- (yellow) or down- (blue) regulation of the transcripts. Genes with significant fold-changes in expression were used to validate microarray results using RT^2-PCR after (B) 6h and (C) 12h of treatment. RT^2-PCR data are averages of three experiments from LSK cells pooled from 20 mice.

Figure 5. TCDD treatment changes the expression of transcripts involved in hematopoietic system development and function.

Data sets containing 35,556 microarray probes were analyzed at 6h and 12h. Transcripts with regulated expression were overlaid onto a global molecular network developed from information contained in the IPA's knowledge base. All relationships are supported by at least one reference from the literature, from a textbook, or from canonical information stored in the IPA's knowledge base. Hematopoietic system development and function was regulated after TCDD-treatment. Association networks of the transcripts regulated in this category after 6h and 12h were generated using IPA. In the graphical representation of the molecular relationships, transcripts are represented as nodes with shapes indicating the function of the expressed protein. The color of the node indicates the up- (red) or down- (green) regulation (fold-changes > 1.5) of the transcripts. The non-color transcripts were present in our dataset, and have a direct relationship with the regulated transcripts. Also, according to IPA's knowledge base, these are categorized within hematopoietic system development and function.

Downloaded from molpharm.aspetjournals.org at ASPET Journals on April 17, 2024

Molecular Pharmacology Fast Forward. Published on July 26, 2011 as DOI: 10.1124/mol.111.071381
This article has not been copyedited and formatted. The final version may differ from this version.

Table 1. Quantitative analysis of engrafted TCDD–treated BM cells shows no difference in the engraftment potential of HSCs.

Donor BM cells were harvested from mice seven days after treatment with TCDD (30 μg/kg) or vehicle (olive oil) by gavage as described in Fig. 2 legend. Repopulated recipients contained > 1% of $CD45.2^+$ cells in total BM cells. The proportions of HSCs per million of BM cells were calculated using the L-Calc Software entering the numbers of total surviving and repopulated mice. Representative results from one of two independent experiments (n=8 recipients per dilution of donor BM cells per group). Pearson's Chi Square p-value = 1 was consistent with a Poisson's distribution of data.

	Short-term (6 weeks)		**Long-term (20 weeks)**	
	Vehicle	**TCDD**	**Vehicle**	**TCDD**
Proportion (HSCs per million BM cells)	13.4	11.0	10.3	6.1
95% Confidence Interval	6.0-30	5.3-22	5.1-21	2.9-13
p-value of Pearson's Chi-Square	0.7966	0.4722	0.9853	0.9507

Downloaded from molpharm.aspetjournals.org at ASPET Journals on April 17, 2024

Molecular Pharmacology Fast Forward. Published on July 26, 2011 as DOI: 10.1124/mol.111.071381
This article has not been copyedited and formatted. The final version may differ from this version.

Table 2. Transcripts consistently up- or down-regulated at 6h and 12h in LSKs after TCDD treatment.

Microarray experiments were performed from LSKs isolated using immuno-magnetic sorting. Hierarchical clustering of microarray results was used to determine groups of genes co-regulated. (n=5 microarrays from pooled samples of 20 mice per group).

		Fold Change (TCDD/Vehicle)	
Gene Symbol	**mRNA Accession Number**	**6h**	**12h**
Scin	NM_001146196	6.4	7.9
Mmp8	NM_008611	4.4	1.8
Il1f9	NM_153511	2.3	4.3
Nqo1	NM_008706	2.2	1.6
Flnb	NM_134080	2.2	1.9
Gm5662	NM_001013824	2.1	3.9
Slamf7	NM_144539	-1.6	-3.2

Downloaded from molpharm.aspetjournals.org at ASPET Journals on April 17, 2024

Table 3. Important biological functions were significantly altered in LSKs 6 and 12 h after TCDD treatment.

A 1.5 cut-off of fold-change (TCDD/vehicle) was set to identify transcripts whose expression was regulated. The top biological functions based in their Fisher's exact test p-value (in brackets) are shown. The numbers in parentheses after the name of the functions are the number of transcripts in our data sets common to the Ingenuity's Knowledge Base reference set.

6h		12h	
Molecular and Cellular Functions			
Cell-To-Cell Signaling and Interaction (23)	[$9.52x10^{-4}$ - $3.92x10^{-2}$]	Antigen Presentation (17)	[$2.11x10^{-8}$ - $4.44x10^{-2}$]
Cellular Movement (9)	[$2.20x10^{-3}$ - $4.48x10^{-2}$]	Cell-To-Cell Signaling and Interaction (16)	[$2.11x10^{-8}$ - $4.89x10^{-2}$]
Antigen Presentation (16)	[$2.51x10^{-3}$ - $3.92x10^{-2}$]	Cellular Movement (14)	[$1.54x10^{-7}$ - $4.44x10^{-2}$]
Cellular Development (19)	[$4.54x10^{-3}$ - $4.31x10^{-2}$]	Cell Death (10)	[$3.65x10^{-6}$ - $4.44x10^{-2}$]
Cell Morphology (4)	[$9.90x10^{-3}$ - $2.67x10^{-2}$]	Cell Signaling (27)	[$9.02x10^{-6}$ - $2.48x10^{-3}$]
Physiological System Development and Function			
Hematological System Development and Function (44)	[$2.79x10^{-5}$ - $4.96x10^{-2}$]	Hematological System Development and Function (26)	[$2.11x10^{-8}$ - $4.89x10^{-2}$]
Tissue Morphology (17)	[$2.79 x10^{-5}$ - $2.67x10^{-2}$]	Immune Cell Trafficking (17)	[$2.11x10^{-8}$ - $4.89x10^{-2}$]

Molecular Pharmacology Fast Forward. Published on July 26, 2011 as DOI: 10.1124/mol.111.071381
This article has not been copyedited and formatted. The final version may differ from this version.

Downloaded from molpharm.aspetjournals.org at ASPET Journals on April 17, 2024

Lymphoid Tissue Structure and Development (10)	[$1.39x10^{-3}$ - $3.92x10^{-2}$]	Hematopoiesis (15)	[$2.75x10^{-7}$ - $4.44x10^{-2}$]
Hematopoiesis (20)	[$2.20x10^{-3}$ - $4.48x10^{-2}$]	Lymphoid Tissue Structure and Development (12)	[$6.22x10^{-5}$ - $2.25x10^{-2}$]
Immune Cell Trafficking (23)	[$2.20x10^{-3}$ - $4.96x10^{-2}$]	Humoral Immune Response (3)	[$1.13x10^{-4}$ - $2.98x10^{-2}$]

Molecular Pharmacology Fast Forward. Published on July 26, 2011 as DOI: 10.1124/mol.111.071381
This article has not been copyedited and formatted. The final version may differ from this version.

Downloaded from molpharm.aspetjournals.org at ASPET Journals on April 17, 2024

Molecular Pharmacology Fast Forward. Published on July 26, 2011 as DOI: 10.1124/mol.111.071381
This article has not been copyedited and formatted. The final version may differ from this version.

Figure 1

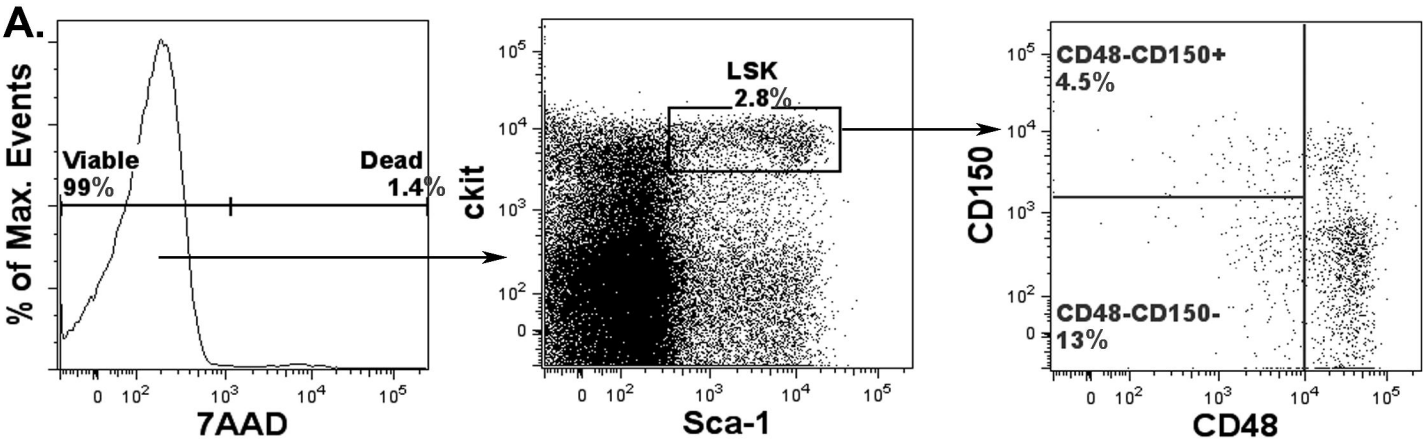

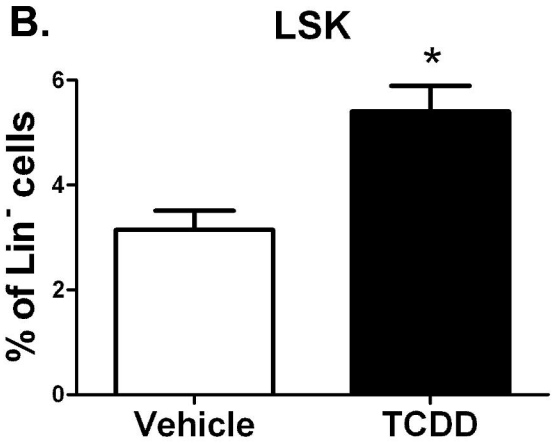

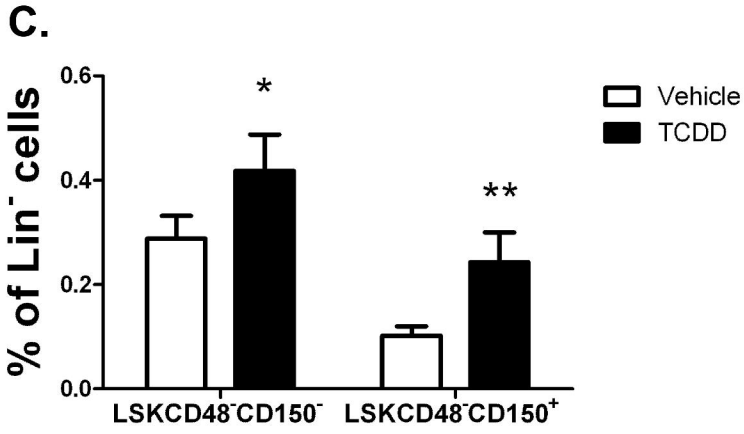

Downloaded from molpharm.aspetjournals.org at ASPET Journals on April 17, 2024

Molecular Pharmacology Fast Forward. Published on July 26, 2011 as DOI: 10.1124/mol.111.071381
This article has not been copyedited and formatted. The final version may differ from this version.

Figure 2

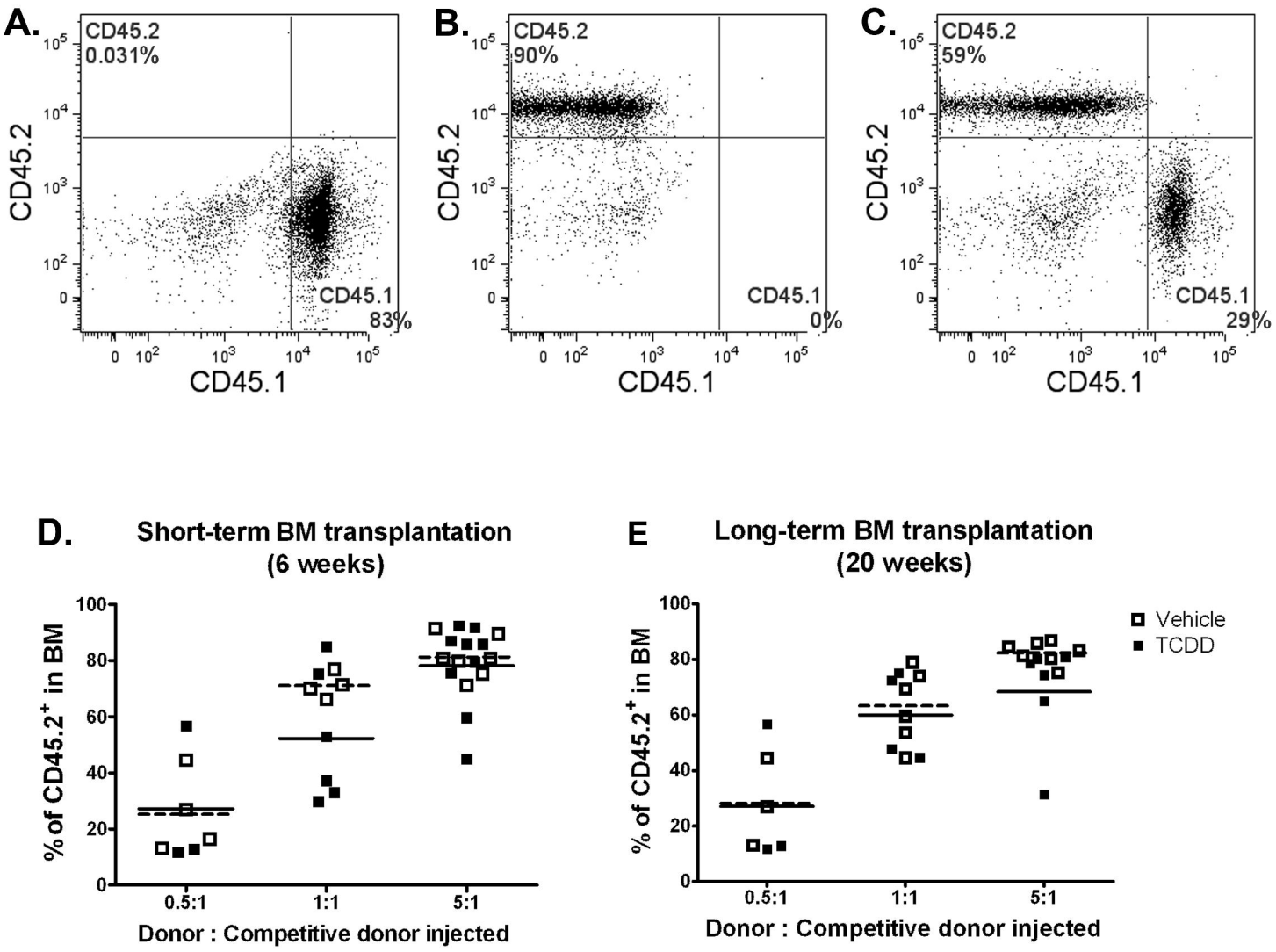

Downloaded from molpharm.aspetjournals.org at ASPET Journals on April 17, 2024

Molecular Pharmacology Fast Forward. Published on July 26, 2011 as DOI: 10.1124/mol.111.071381
This article has not been copyedited and formatted. The final version may differ from this version.

Figure 3

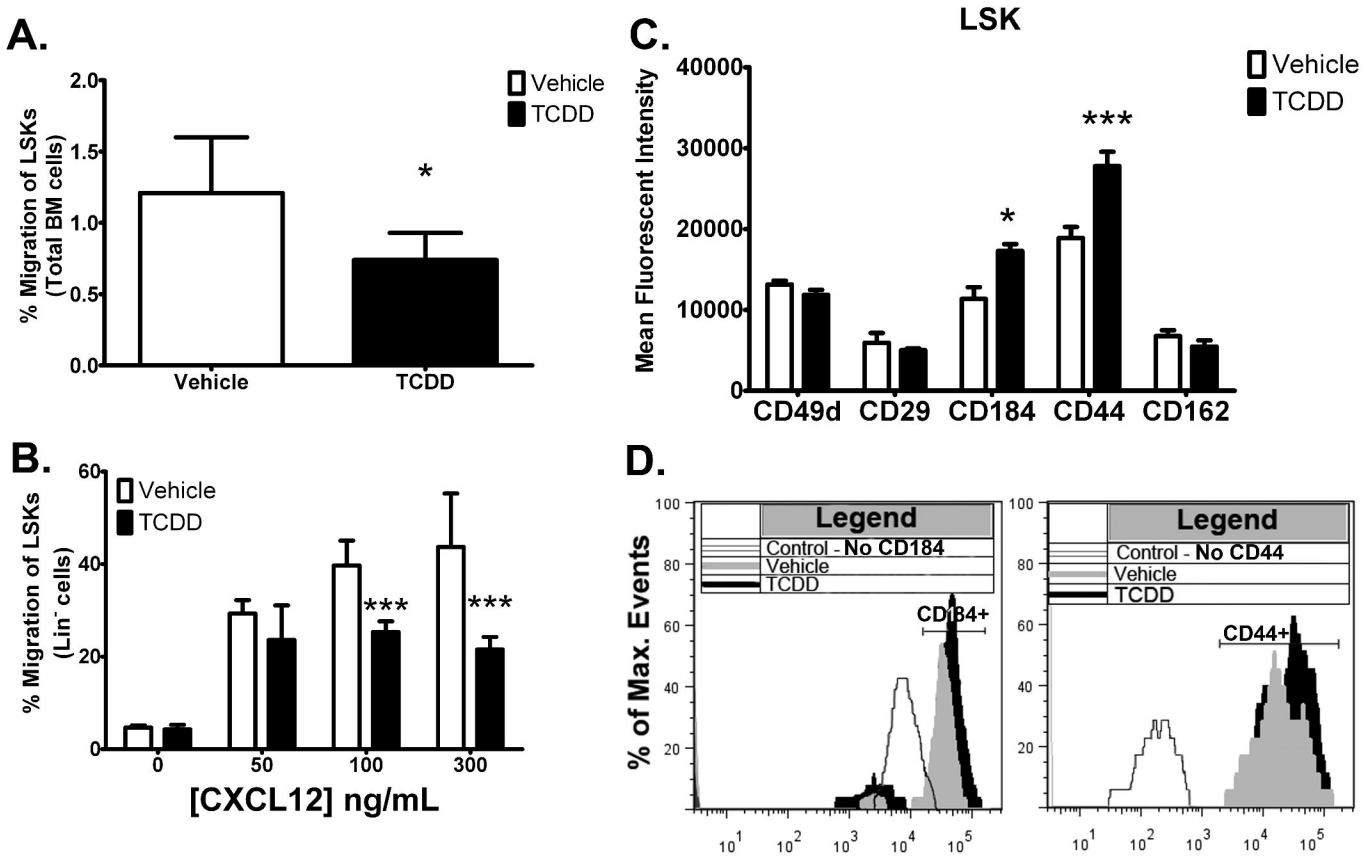

Downloaded from molpharm.aspetjournals.org at ASPET Journals on April 17, 2024

Figure 4.

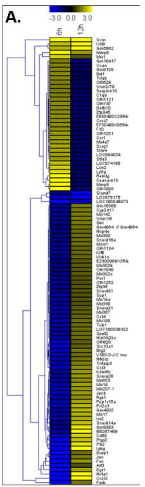
A.
-3.0 0.0 3.0

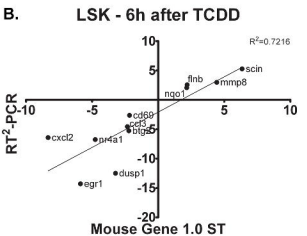
B.
LSK - 6h after TCDD
R2=0.7216
RT2-PCR
Mouse Gene 1.0 ST
scin
flnb
mmp8
nqo1
cd69
cxcl2
pr4a1
dusp1
egr1

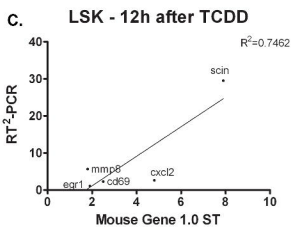
C.
LSK - 12h after TCDD
R2=0.7462
RT2-PCR
Mouse Gene 1.0 ST
scin
mmp8
cxcl2
egr1
cd69

Figure 5

A. LSK - TCDD 6h

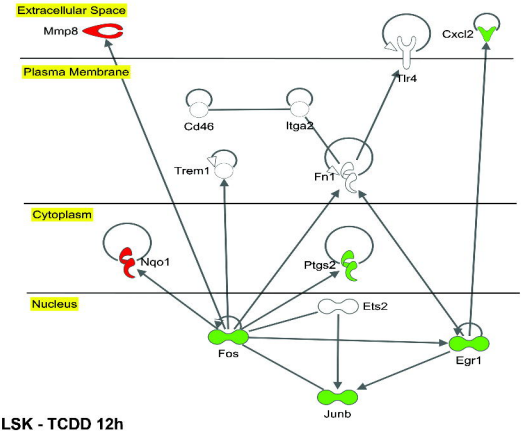

B. LSK - TCDD 12h

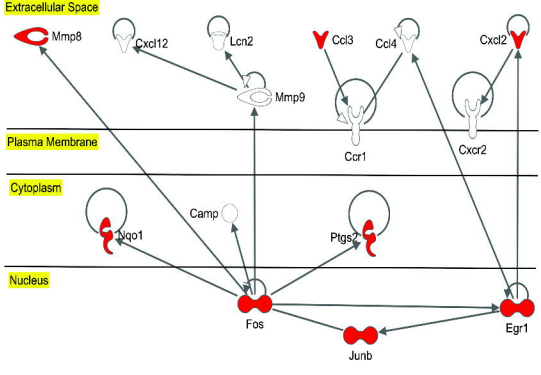

Aryl hydrocarbon receptor activation in hematopoietic stem/progenitor cells alters cell function and pathway-specific gene modulation reflecting changes in cellular trafficking and migration

Fanny L. Casado, Kameshwar P. Singh, Thomas A. Gasiewicz.

Molecular Pharmacology

Supplemental Figure S1. LSK cells were obtained from mice treated with TCDD (30 µg/kg, 7d) or vehicle. Cells were cultured as described in Materials and Methods. Cells were harvested after 7d (A and B) or 14 d (C and D). Phenotypic characterization of Lin^- and Lin^+ sub-populations were performed using flow cytometry as previously described (Singh et al., 2009). MPP, multipotent progenitors; CLP, common lymphoid progenitors. Bar graphs represent averages from three wells.

Supplemental Figure S2. Lin^- cells from mice treated with TCDD (30 µg/kg, 7d) or vehicle were analyzed for apoptosis as described in Materials and Methods. Cumulative data for the (A) viable and (B) apoptotic LSK cells are shown. Results are representative of one experiment with six replicate mice. Squares represent values for individual mice. Average values for vehicle and TCDD groups are represented by dashed and solid lines, respectively.

Supplemental Table S1. Gene-specific primers were used to validate results provided by microarray experiments.

Genes with fold-changes higher than 2 and p-values lower than 0.05 were used to validate microarray results using RT^2-PCR after 6h and 12h of treatment. RT^2-PCR was performed using commercially available probe and primer sets (SA Biosciences).

Gene Symbol	mRNA Accession	RT^2 qPCR Primer Assay for Mouse
Btg2	NM_007570	PPM-04999A
Ccl3	NM_011337	PPM-02949E
Cd69	NM_001033122	PPM-03243E
Cxcl2	NM_009140	PPM-02969E
Dusp1	NM_ 013642	PPM-04529A
Egr1	NM_007913	PPM-02938B
Flnb	NM_134080	PPM-27183A
Gapdh	NM_008084	PPM-02946E
Hprt1	NM_013556	PPM-03559E
Mmp8	NM_008611	PPM-03610B
Nqo1	NM_008706	PPM-03466E
Nr4a1	NM_010444	PPM-24496A
Scin	NM_001146196	PPM-24799A

Supplemental Table S2. A set of transcripts was up-regulated in LSKS after 6h of *in vivo* TCDD (30 μg/kg) treatment but not 6h later.

Total RNA was obtained from sorted LSK cells. Fold-changes in normalized values of gene expression for TCDD or vehicle control groups were calculated using microarray technology. Microarray data represent averages of five experiments using RNA from LSKs pooled from 20 mice per treatment.

		Fold Change [TCDD/Vehicle]	
Gene Symbol	**mRNA Accession Number**	**6h**	**12h**
Olfr1095	NM_146730	4.6	-1.2
Mmp9	NM_013599	4.4	-1.1
Ceacam10	NM_007675	3.7	-1.1
Retnlg	NM_181596	3.1	-1.1
Msr1	NM_031195	2.5	1.0
Lcn2	NM_008491	2.4	-1.1
Slfn4	NM_011410	2.0	-1.2
Scrg1	NM_009136	2.0	-1.1
Stfa3	NM_025288	1.8	-1.3
Ms4a7	NM_027836	1.8	-1.1
Olfr1251	NM_001011529	1.8	-1.1

Ccr1	NM_007721	1.8	-1.1
Cxcr2	NM_009909	1.7	-1.1
5730408K05Rik	NR_027866	1.7	-1.1
F10	NM_007972	1.7	-1.1
Olfr747	NM_207156	1.6	-1.3
Olfr1121	NM_146348	1.6	-1.3
Zfp345	NM_001034900	1.6	-1.2
Defb10	NM_139225	1.6	-1.2
Gm8109	XR_001873	1.6	-1.1
Vcan	NM_001081249	1.6	-1.1
Tifab	NM_001168615	1.6	-1.0
Bst1	NM_009763	1.6	-1.0
C1qb	NM_009777	1.5	-1.2
Vmn2r79	NM_001105190	1.5	-1.1
Serpinb10	NM_198028	1.5	-1.1
Olfr628	NM_147097	1.5	-1.0

Supplemental Table S3. A set of transcripts was down-regulated in LSKs after 6h of *in vivo* TCDD treatment (30 μg/kg) but up-regulated 6h later.

Total RNA was obtained from sorted LSK cells. Fold-changes in normalized values of gene expression for TCDD or vehicle control groups were calculated using microarray technology. Microarray data represent averages of five experiments using RNA from LSKs pooled from 20 mice per treatment.

		Fold Change [TCDD/Vehicle]	
Gene Symbol	**mRNA Accession Number**	**6h**	**12h**
Cxcl2	NM_009140	-8.4	4.8
Egr1	NM_007913	-5.9	1.9
Nr4a1	NM_010444	-4.7	3.9
Fos	NM_010234	-4.2	1.8
Jun	NM_010591	-3.5	1.5
Plk2	NM_152804	-3.1	2.7
Ptgs2 (Cox2)	NM_011198	-2.7	2.3
Ighg	X70423	-2.7	3.0
Ccl3	NM_011337	-2.3	1.7
Cd69	NM_001033122	-2.2	2.5
Prl2c3	NM_011118	-2.1	2.2

Ppp1r15a (Myd116)	NM_008654	-2.1	2.0
Rgs1	NM_015811	-2.1	1.7
Mir297-1	NR_029647	-2.0	1.8
Junb	NM_008416	-2.1	1.8
Tnfaip3	NM_009397	-2.0	1.5
Mir18	NR_030534	-2.0	1.9
Mir653	NR_030612	-1.9	1.7
BB287469	NM_001177573	-1.8	3.0
Mir17	NR_029785	-1.8	2.1
Gm4005	XM_001476146	-1.8	2.2
Ier2	NM_010499	-1.8	2.0
Gm16368	ENSMUST00000095505	-1.7	1.5
Cyp2d11	NM_001104531	-1.7	1.5
Kdm6b	NM_001017426	-1.7	1.8
Snora28	NR_033168	-1.7	1.8
Mir142	NR_029555	-1.6	1.5
Gm8393	XR_033884	-1.6	2.7
Snord14a	NR_028273	-1.5	2.3
Vmn1r6	NM_134175	-1.5	1.5

Supplemental Table S4. A set of transcripts was down-regulated in LSKs after 6h of *in vivo* TCDD treatment (30 μg/kg) but not 6h later.

Total RNA was obtained from sorted LSK cells. Fold-changes in normalized values of gene expression for TCDD or vehicle control groups were calculated using microarray technology. Microarray data represent averages of five experiments using RNA from LSKs pooled from 20 mice per treatment.

		Fold Change [TCDD/Vehicle]	
Gene Symbol	**mRNA Accession Number**	**6h**	**12h**
Fosb	NM_008036	-10.7	1.4
Atf3	NM_007498	-4.8	1.0
Dusp1	NM_022019	-3.2	1.3
Slc10a1	NM_001177561	-2.4	1.2
Btg2	NM_007570	-2.2	1.4
Olfr820	NM_146675	-2.2	1.1
V165-D-J-C mu	ENSMUST00000103526	-2.1	1.3
Nfkbiz	NM_030612	-2.0	1.4
Spp1	NM_009263	-1.9	1.0
Trib1	NM_144549	-1.9	1.3
Mir190	NR_030543	-1.9	1.3
Ccl4	NM_013652	-1.9	1.2
Hist1h2bc	NM_023422	-1.8	1.3

Spef2	NM_177123	-1.8	1.3
LOC100038422	AK137634	-1.8	1.3
Mir367	NR_030268	-1.8	1.1
Mir19a	NR_029786	-1.8	1.0
Snora31	NR_028481	-1.7	1.1
Mir340	NR_029769	-1.7	1.0
Snord61	NR_002903	-1.6	1.0
Zfp36	NM_011756	-1.6	1.0
Klrb1c	NM_001159904	-1.6	1.2
Olfr1252	NM_207568	-1.6	1.0
Klf6	NM_011803	-1.6	1.2
Mcrs1	NM_016766	-1.6	1.3
Olfr1134	NM_147030	-1.6	1.2
Nlrp4e	NM_001004194	-1.5	1.3
Snord16a	NR_028548	-1.5	1.3
Olfr1049	NM_147016	-1.5	1.1
Skil	NM_011386	-1.5	1.4
Mir380	NR_029881	-1.5	1.3
Mir302b	NR_030403	-1.5	1.1
Mir302c	NR_030404	-1.5	1.1
Per1	NM_001159367	-1.5	1.0

Supplemental Table S5. List of transcripts regulated in LSKs after 6h and 12 h of *in vivo* TCDD treatment (30 μg/kg) for the most relevant molecular and cellular functions.

Transcripts with fold-changes (TCDD/vehicle) > 1.5 were ranked based in their Fisher's exact test p-value. The transcripts in the datasets common to specific categories within the Ingenuity's Knowledge Base reference set are shown here.

6h	12h
Cell-To-Cell Signaling and Interaction: *C3ar1, Ccl3, Cd69, Cd200, Cd209a, Clec4b2, Cnr2, Csf2rb, Cxcl2, Fn1, Gzma, Hspa1a, Il1a, Ikbkb, Klrd1, Klrk1, Ltb, Pf4, Pros1, Ptgs2, Sele, Tlr4, Trem1*	Antigen Presentation *C5ar1, Camp, Ccl3, Ccl4, Ccr1, Cd69, Cxcl2, Cxcl12, Cxcr2, Fpr1, Irf4, Lcn2, Ltf, Mmp9, Msr1, Ptgs2, Spp1*
Cellular Movement *Ccl3, Cnn2, Cxcl2, Fn1, Pf4, Saa1, Sele, St3gal4, Tlr4*	Cell-To-Cell Signaling and Interaction *C5ar1, Camp, Ccl3, Ccl4, Ccr1, Cd69, Cxcl2, Cxcl12, Cxcr2, Fpr1, Lcn2, Ltf, Mmp9, Msr1, Ptgs2, Spp1*
Antigen Presentation *Cd200, Cnn2, Cxcl2, Cxcr6, Fn1, Grap2, Havcr1, Ikbkb, Il1a, Pf4, Pros1, Ptger2, Ptgs2, Sele, Tek, Tlr4*	Cellular Movement *Camp, Ccl3, Ccl4, Cxcr2, Cxcl2, Cxcl12, Ccr1, F10, Fpr1, Igh-6, Ptgs2, Msr1, Mmp9, Spp1*
Cellular Development *Atrn, Cnn2, Cnr2, Csf2rb, Egr1, Ets2, Fn1, Fos, Ifi16, Igh-6, Ikbkb, Il1a, Irf4, Junb,*	Cell Death *Camp, Cxcl12, Fcer1a, Jun, Lepr, Ltf, Mmp8, Mmp9, Msr1, Nr4a1*

Klrd1, Lifr, Pf4, Tlr4, Trem1	
Cell Morphology *Atrn, Cnn2, Fn1, Sele*	Cell Signaling *Camp, Ccl3, Ccl4, Cxcl2, Cxcl12, Fcer1a, Fpr1*

Supplemental Table S6. List of transcripts regulated in LSKs after 6h and 12 h of *in vivo* TCDD treatment (30 μg/kg) for the most relevant physiological systems and functions.

Transcripts with fold-changes (TCDD/vehicle) > 1.5 were ranked based in their Fisher's exact test p-value. The transcripts in the datasets common to specific categories within the Ingenuity's Knowledge Base reference set are shown here.

6h	12h
Hematological System Development and Function *C3ar1, Ccl3, Cd46, Cd69, Cd200, Cd209, Clec4b2, Cnn2, Cnr2, Csf2rb, Cxcl2, Cxcr6 Egr1, Ets2, Fn1, Fos, Grap2, Grn, Gzma, Havcr1, Hspa1a, Ier3, Ifi16, Ikbkb, Il1a, Irf4, Itga2, Junb, Klrd1, Klrk1, Lifr, Ltb, Mmp8, Nqo1, Nqo2, Pf4, Pros1, Ptger2, Ptgs2, Sele, St3gal4, Tek, Tlr4, Trem1*	Hematological System Development and Function *C5ar1, Camp, Ccl3, Ccl4, Ccr1, Cd69, Cd74, Cxcl2, Cxcl12, Cxcr2, Dusp1, Egr1, Fos, Fpr1, Igh-6, Irf4, Junb, Lcn2, Ltf, Mmp8, Mmp9, Msr1, Nqo1, Plscr1, Ptgs2, Spp1*
Tissue Morphology *Cd200, Cnn2, Cnr2, Cxcr6, Grap2, Havcr1, Ikbkb, Il1a, Irf4, Junb, Mmp8, Nqo1, Nqo2, Ptger2, Sele, Tek, Tlr4*	Immune Cell Trafficking *C5ar1, Camp, Ccl3, Ccl4, Ccr1, Cxcl2, Cxcl12, Cxcr2, F10, Fpr1, Igh-6, Lcn2, Ltf, Mmp9, Msr1, Ptgs2, Spp1*
Lymphoid Tissue Structure and Development *Cnn2, Cnr2, Cxcl2, Il1a, Mmp8, Nqo1,*	Hematopoiesis *Camp, Ccl3, Ccl4, Ccr1, Cd74, Cxcl2, Cxcl12, Cxcr2, Egr1, F10, Fos, Fpr1, Irf4,*

Nqo2, Pf4, Sele, Tlr4	*Junb, Mmp9*
Hematopoiesis *Ccl3, Cnn2, Cnr2, Csf2rb, Cxcl2, Egr1, Ets2, Fn1, Fos, Ifi16, Ikbkb, Irf4, Junb, Lifr, Pf4, Saa1, Sele, St3gal4, Tlr4, Trem1*	Lymphoid Tissue Struct. and Development *C5ar1, Camp, Ccl3, Ccl4, Cxcl2, Cxcr2, Egr1, Fpr1, Mmp8, Mmp9, Nqo1, Plscr1,*
Immune cell Trafficking *C3ar1, Ccl3, Cd200, Clec4b2, Cnn2, Cxcl2, Ets2, Fn1, Grn, Gzma, Hspa1a, Ier3, Ikbkb, Il1a, Itga2, Pf4, Pros1, Ptgs2, Saa1, Sele, St3gal4, Tlr4, Trem1*	Humoral Immune Response *Ccl4, Cxcl12, Fpr1*

Supplemental Figure 1

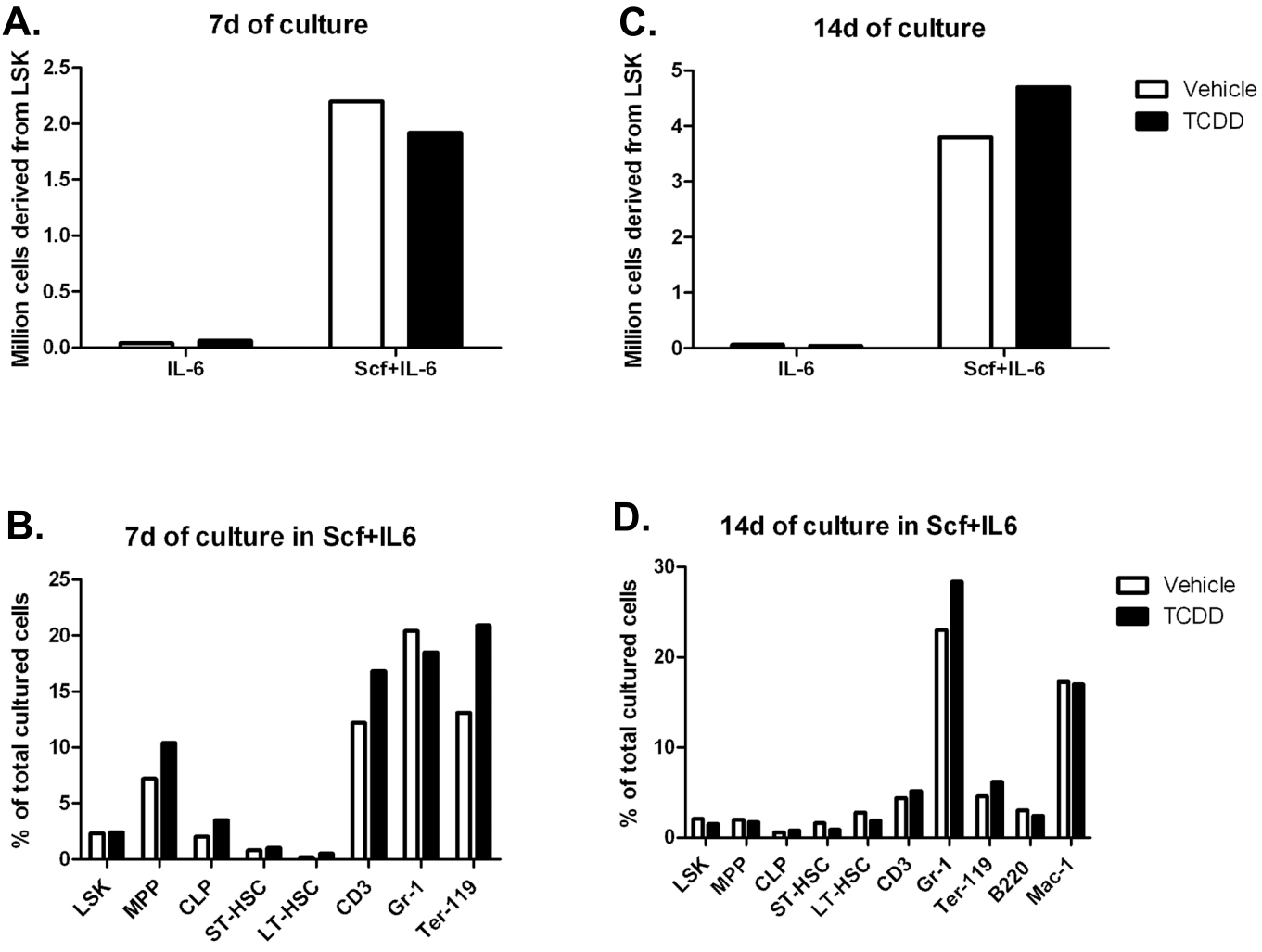
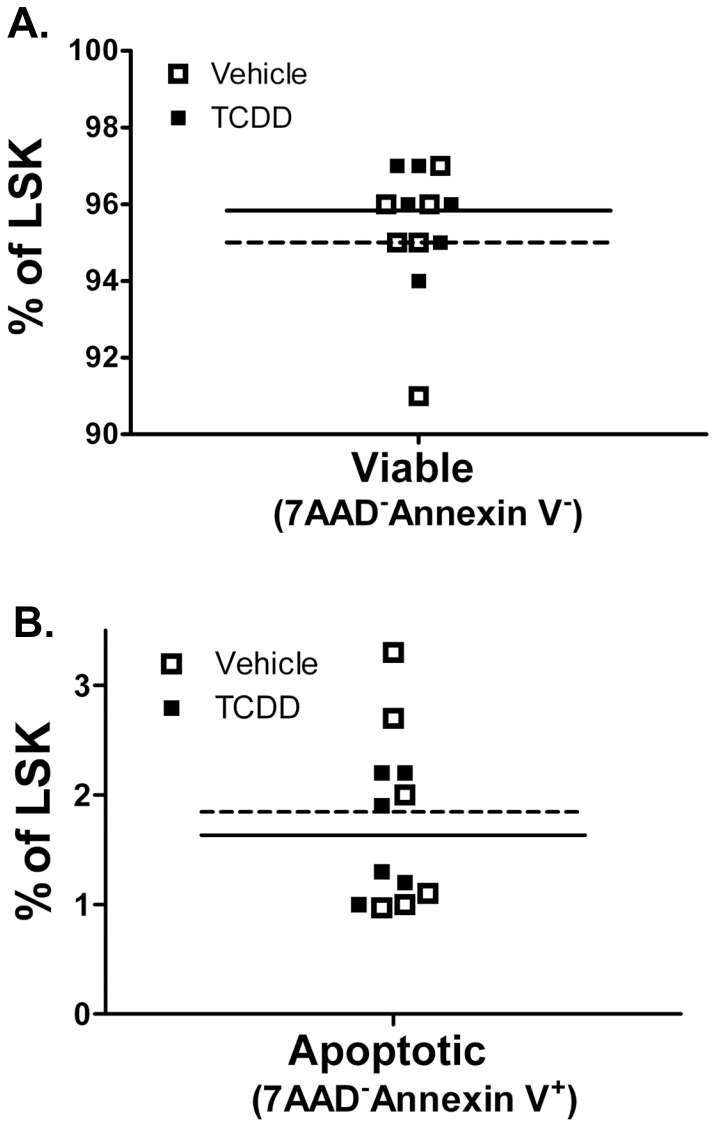
Supplemental Figure 2